NASA Technical Memorandum 112200

Exact Solutions for Sound Radiation from a Circular Duct

Y. C. Cho, Ames Research Center, Moffett Field, California
K. Uno Ingard, Massachusetts Institute of Technology, Cambridge, Massachusetts

June 1997

National Aeronautics and
Space Administration

Ames Research Center
Moffett Field, California 94035-1000

EXACT SOLUTIONS FOR SOUND RADIATION FROM A CIRCULAR DUCT*

Y. C. Cho and K. Uno Ingard†

Ames Research Center

SUMMARY

This paper presents a method of evaluation of Wiener-Hopf technique solutions for sound radiation from an unflanged circular duct with infinitely thin duct wall, including mean flows.

1. INTRODUCTION

Sound radiation from circular ducts is a classical acoustics problem. Exact solutions were previously reported: the Wiener-Hopf technique was used for radiation of propagating modes from a circular duct with negligibly thin duct wall (refs. 1–3), and the hyperboloidal wave function was defined and employed for radiation from duct with various types of termination, including a plane flange and horns (ref. 4). Exact solutions undoubtedly help one to gain physical insight into the problem and can often be used in practical designs. In this electronic computation age, another significant role of exact solutions is defined as means of cross examination of results of numerical techniques. These techniques, embraced as computational aeroacoustics, are just starting to attract widespread attention as a potential tool in attacking important aeroacoustic problems for which quantitative solutions are not available.

Despite the elegance of the closed form solutions with the Wiener-Hopf technique, numerical presentations have been limited to mere demonstrations of its capability. As a matter of fact, no computer program is publicly available for its numerical evaluation. Numerical evaluation of the Wiener-Hopf solution is not straightforward; it requires the exercise of extreme care and, often, sophisticated mathematical tricks. This paper attempts to provide a comprehensive mathematical procedure for evaluation of Wiener-Hopf solutions.

In section 2, acoustic waves will be briefly reviewed for in-duct propagation and radiation. In section 3, the Wiener-Hopf technique is applied to obtain solutions, and section 4 is devoted to the evaluation of integrals involved in the solutions.

---

*Partly based on two consulting reports submitted to Pratt and Whitney Aircraft, May 25, 1976, and December 17, 1976.

†Massachusetts Institute of Technology, Cambridge, Massachusetts.

2. REVIEW OF DUCT ACOUSTICS

Duct acoustics will be briefly reviewed here for aspects relevant to the present problem. This review is also intended for clarification of terminology and nomenclature used in this paper.

The wave equation for the acoustic pressure, p, in flow is

$$\nabla^2 p - \frac{1}{c^2}\left(\frac{\partial}{\partial t} + \bar{V}\cdot\bar{\nabla}\right)^2 p = 0 \tag{1}$$

Here c is speed of sound, and $\bar{V}$ the mean flow velocity which is assumed to have only the axial component. The analysis is confined to a steady wave with the harmonic time dependence $e^{-i\omega t}$, and axial angle dependence $e^{im\phi}$, where m is an integer called the circumferential mode number. Equation (1) is then written for circular cylindrical coordinates (r, ϕ, x) as

$$\frac{1}{r}\frac{\partial}{\partial r}\left(r\frac{\partial p}{\partial r}\right) + \frac{\partial^2 p}{\partial x^2} + \left(k + iM\frac{\partial}{\partial x}\right)^2 p - \frac{m^2}{r^2}p = 0 \tag{2}$$

where $k = \omega/c$ and $M = V/c$.

The sound radiation from an unflanged circular duct is schematically displayed in figure 1. With reference to this figure, the entire region is divided into two: region 1 for $r < a$, and region 2 for $r > a$, where a is the duct radius. The subscripts 1 and 2 will be used from now on to indicate, respectively, regions 1 and 2, unless specified otherwise. The mean flow velocities are assumed to be uniform in each region and are denoted by V_1 and V_2. For $V_1 \neq V_2$, there will be the mean flow mismatch at $r = a$, for $x > 0$. The sound speed can differ for the two regions for reasons such as differences in mean density and temperature. The respective sound speeds, wave constants, air densities, and Mach numbers are denoted by c_1 and c_2, k_1 and k_2, ρ_1 and ρ_2, and M_1 and M_2, where $k_1 = \omega/c_1$, $k_2 = \omega/c_2$, $M_1 = V_1/c_1$, and $M_2 = V_2/c_2$.

In a hard-wall circular duct, the general solution to equation (2) is obtained as

$$p(r,x) = \sum_{n=1}^{\infty} J_m\left(\frac{\mu_{mn} r}{a}\right)\left\{A_{mn} e^{ik_{mn}^{+} x} + B_{mn} e^{ik_{mn}^{-} x}\right\} \tag{3}$$

Here J_m is the Bessel function of order m, μ_{mn} the nth zero of $J_m'(x)$, and A_{mn} and B_{mn} constant coefficients. The wave constants k_{mn}^{+} and k_{mn}^{-} correspond to the mode propagations, respectively, in the positive (to the right) and the negative (to the left) directions, and are given by

$$k_{mn}^{\pm} = \frac{-k_1 M_1 \pm \sqrt{k_1{}^2 - \left(1 - M_1^2\right)\left(\frac{\mu_{mn}}{a}\right)^2}}{1 - M_1^2} \tag{4}$$

The integer n here is called the radial mode number, and the pair (m,n) is used to represent a single duct mode.

Consider the incident wave of a single mode, say (m,ℓ),

$$p_{inc} = J_m\left(\frac{\mu_{m\ell}\, r}{a}\right) e^{i m \varphi} e^{i k_{m\ell}^{+} x} \tag{5}$$

This wave is incident from $x=-\infty$ and propagating toward duct termination, as shown in figure 1. Upon arriving at the duct termination, it will be partly reflected back into the duct and partly radiated out of the duct. In general, the reflected wave contains many radial modes, including propagating and attenuating modes, and is represented by

$$p_{refl} = e^{im\phi} \sum_{n=1}^{\infty} R_{\ell,n}^{m} J_m\left(\frac{\mu_{mn}\, r}{a}\right) e^{i k_{mn}^{-} x} \tag{6}$$

Here $R_{\ell,n}^{m}$ is the conversion coefficient for the (m,ℓ) mode incident and the (m,n) mode reflected. The reflection problem is completely solved by determining this coefficient for all values of n. The Wiener-Hopf technique yields radiation solutions in terms of the far field, which is represented by

$$p_{rad} = e^{im\phi} f_{m\ell}(\theta) \cdot \frac{1}{k_2 R} e^{i \Lambda(k_2, M_2, R)} \tag{7}$$

Here R is the radial distance from the center of the duct termination and θ the polar angle measured from the x-axis (duct axis), as shown in figure 1. (R,θ,ϕ) are spherical coordinates. The complex factor $f_{m\ell}(\theta)$ is called the amplitude gain function, which provides the far field directivity of radiation. The phase $\Lambda(k_2, M_2, R)$ of the far field depends on M_2 as well as on k_2 and R. The radiation problem is completely solved by determining $f_{m\ell}(\theta)$ and $\Lambda(k_2, M_2, R)$.

This analysis with a single mode incident can be extended to accommodate incident waves composed of many modes in a straightforward manner.

3. WIENER-HOPF FORMULATION

The Wiener-Hopf technique involves extensive mathematical manipulation in the Fourier transform space. The Fourier transform of $p(r, x)$ is given by

$$\Phi(r,\alpha)=\frac{1}{\sqrt{2\pi}}\int_{-\infty}^{\infty} p(r,x)\mathrm{e}^{i\alpha x}\mathrm{d}x \tag{8}$$

and $p(r, x)$ is restored by the inverse transform

$$p(r,x)=\frac{1}{\sqrt{2\pi}}\int_{-\infty}^{\infty} \Phi(r,\alpha)\mathrm{e}^{-i\alpha x}\mathrm{d}\alpha \tag{9}$$

In the process of the Wiener-Hopf formulation, various parameters and functions are defined and derived as follows:

$$\gamma_j(\alpha)=\sqrt{1-M_j}\,\sqrt{\left(\alpha-q_j^-\right)\cdot\left(\alpha-q_j^+\right)},\quad q_j^{\pm}=\frac{\pm k_j}{1\mp M_j}\quad \text{for } j=1,2 \tag{10}$$

$$W_1(\alpha)=\frac{I_m(\gamma_1 a)}{\gamma_1 a\, I_m'(\gamma_1 a)},\ I_m \text{ being } I-\text{Bessel function of order } m \tag{11}$$

$$W_2(\alpha)=\frac{K_m(\gamma_2 a)}{\gamma_2 a\, K_m'(\gamma_2 a)},\ K_m \text{ being } K-\text{Bessel function of order } m \tag{12}$$

$$T_M=\frac{1}{\sqrt{1-M_1^2}}\left[\frac{\rho_1 c_1^2 M_1^2}{\sqrt{1-M_1^2}}+\frac{\rho_2 c_2^2 M_2^2}{\sqrt{1-M_2^2}}\right] \tag{13}$$

$$K(\alpha)=\frac{a}{T_M\gamma_1}\left[\rho_1 c_1^2\left(k_1+\alpha M_1\right)^2 W_1(\alpha)-\rho_2 c_2^2\left(k_2+\alpha M_2\right)^2 W_2(\alpha)\right] \tag{14}$$

In deriving $K(\alpha)$, we have used the condition of the continuity of the acoustic pressure and acoustic displacement at the mean flow mismatch at $r = a$, for $x > 0$. $K(\alpha)$ is factorized into two: one is analytic in the upper half plane (+) and the other in the lower half plane (–) as $K(\alpha)=K_+(\alpha)\cdot K_-(\alpha)$. These factors will be included in the final solutions with arguments representing physical quantities. For the present problem, the factorization is obtained not in closed forms but in integral representations as follows:

$$\mathrm{Log}\,K_+(y_+)=\frac{1}{2\pi i}\int_{C_+}\frac{\mathrm{Log}\,K(\alpha)}{\alpha-y_+}\mathrm{d}\alpha \tag{15}$$

$$\mathrm{Log}\,K_-(y_-)=\frac{-1}{2\pi i}\int_{C_-}\frac{\mathrm{Log}\,K(\alpha)}{\alpha-y_-}\mathrm{d}\alpha \tag{16}$$

Here the integral path is from $-\infty$ to $+\infty$ near the real axis, and the argument y_+ (y_-) is located above (below) the respective integral path, as illustrated in figure 2.

Forgoing details of the formulation (ref. 5), the final results are presented here. The conversion coefficient for the reflection is obtained as

$$R_{\ell,n}^{m} = \frac{i\rho_1 c_1^{\,2}}{a T_M \sqrt{1-M_1^{\,2}}} \cdot \frac{J_m(\mu_{m\ell})}{J_m(\mu_{mn})} \cdot \left(1-\frac{m^2}{\mu_{mn}^2}\right)^{-1} \left[\left(k_{m\ell}^{+}+\frac{k_1}{1-M_1}\right)\cdot\left(-k_{m\ell}^{-}+\frac{k_1}{1+M_1}\right)\right]^{-1/2}$$

$$\cdot \frac{(k_1-M_1 k_{mn}^{-})^{\,2}}{(k_{m\ell}^{+}-k_{mn}^{-})\left(k_1 M_1+\left(1-M_1^{\,2}\right)k_{mn}^{-}\right)} \cdot \left[K_{-}(-k_{m\ell}^{+})\,K_{+}(-k_{mn}^{-})\right]^{-1} \tag{17}$$

The symmetry between the radial mode numbers ℓ and n is salient, implying that the result satisfies the reciprocity principle (ref. 6), which can be used to infer the conversion coefficients of a nonpropagating mode.

For the radiation, the phase is obtained as

$$\Lambda(k_2, M_2, R) = \frac{k_2}{\sqrt{1-M_2^{\,2}}}\left(R-\frac{M_2 x}{\sqrt{1-M_2^{\,2}}}\right) \tag{18}$$

and the amplitude gain function is

$$f_{m\ell}(\theta) = \frac{(-i)^{m+1} J_m(\mu_{m\ell})\rho_2 c_2^2 k_2^2 \left(1-M_2\cos\theta'\right)^2}{\pi T_M \left(1-M_2^{\,2}\right)^{5/2}} \cdot \left[\sin\theta \cdot H_m^{(1)'}\left(\frac{k_2 a \sin\theta'}{\sqrt{1-M_2^{\,2}}}\right)\right]^{-1}$$

$$\cdot\left\{K_{+}(-\eta(\theta))\cdot\left[k_{m\ell}^{+}-\eta(\theta)\right]\cdot\sqrt{\left(\frac{k_1}{1+M_1}-\eta(\theta)\right)}\cdot K_{-}\left(-k_{m\ell}^{+}\right)\cdot\sqrt{\left(k_{m\ell}^{+}+\frac{k_1}{1-M_1}\right)}\right\}^{-1} \tag{19}$$

where

$$\eta(\theta) = \frac{k_2(\cos\theta'-M_2)}{1-M_2^{\,2}} \tag{20}$$

Here the modified coordinates R' and θ' are defined as

$$R' = \sqrt{r^2+\frac{x^2}{1-M_2^{\,2}}}, \quad \tan\theta' = \sqrt{1-M_2^{\,2}}\tan\theta \tag{21}$$

$H_m^{(1)}(x)$ is the Hankel function of the first kind, and $H_m^{(1)'}(x)$ is its derivative with respect to x.

Comments are made on the expression of $f_{m\ell}(\theta)$ for two limiting cases. First, as can be shown readily, when θ becomes zero, the quantity in the first square bracket will be infinite except for the case of $m = 0$. In other words, the radiated field is zero for $\theta = 0$ except for the radiation of axisymmetric modes. Second, as will be seen later, when its argument approaches $-k_{mn}^+$, K_+ in the second square bracket varies as $[k_{m\ell}^+ - \eta(\theta)]^{-1}$. It follows that the radiated field will be zero for the angle satisfying

$$\eta(\theta)=k_{mn}^+ \quad \text{or} \quad \cos\theta' = M_2 + \left(1-M_2^2\right)\frac{k_{mn}^+}{k_2}, \quad \text{for } n\neq\ell \tag{22}$$

However, for the angle corresponding to the incident propagation constant $k_{m\ell}^+$, the radiated field is nonzero, because the term adjacent to K_+ becomes zero in this limit. In fact, the radiated field reaches the maximum in this limit. These findings are all familiar for cases of no mean flows. We will also see later that if its argument approaches $-k_1/(1+M_1)$, then K_+ varies in such a way as to compensate the term involving the square root in the same square bracket to maintain the amplitude gain finite.

A remark should be made on the constant T_M. As M_1 and M_2 both become zero, this constant becomes zero, but the expressions for the conversion coefficients and the radiation directivity remain correct, and finite when evaluated as a limit.

4. NUMERICAL EVALUATION

The integrals in equations (15) and (16) cannot be carried out analytically, and thus we will employ a semi-numerical method. To this end, all the variables are made dimensionless by multiplying or dividing with the duct radius a. For notation simplification, the sub- or superscript m will often be dropped.

$K(\alpha)$ satisfies all the conditions required for its factorization by the integration. Nevertheless, the integrand possesses singular points in the vicinity of the integral paths. These singular points arise as branch points, simple poles, and zeroes of $K(\alpha)$. It should be emphasized that there are no other singularities near the integral paths. The branch points are located at $\alpha = q_1^{\pm}$. We adopt a rule for determining phase around these branch points, as illustrated in figure 3. For example, consider $(\alpha - q_1^-)$. Its phase is 180 degrees for its real part less than zero, and changes clockwise to zero as the real part becomes positive. On the other hand, the phase of $(\alpha - q_1^+)$ is -180 degrees for the real part less than zero, and changes counterclockwise to zero as the real part becomes positive. This rule should be strictly observed for the integrations.

The simple poles of $K(\alpha)$ occur at zeroes of $I_m'(\gamma_1 a)$, which is included through $W_1(\alpha)$ as in equations (11) and (14). Theses zeroes correspond to the wave constants of duct modes, and one can

show that the simple poles of $K(\alpha)$ are located at $\alpha = v_n^{\pm} \equiv -k_{mn}^{\mp}$. Note that v_n^+ $(\equiv -k_{mn}^-)$ is above the respective integral path, and v_n^- $(\equiv -k_{mn}^+)$ is below the respective integral path, as shown in figure 2. $K(\alpha)$ can also possess zeroes near the integral path if $q_1^+ > q_2^+$. The zeroes are located between $\alpha = q_2^+$ and $\alpha = q_1^+$, and above the integral path. The number of zeroes equals that of simple poles between $\alpha = q_2^+$ and $\alpha = q_1^+$, or can be less by one. The zeroes are denoted by z_n, for $n = 1, 2, \ldots n_o$, with n_o being the number of zeroes. These zeroes are ordered such that z_1 is the smallest and z_{n_o} the largest.

The imaginary parts of all the singular points are related to $\mathcal{Im}(k)$. As the latter tends to zero, all the singular points approach the real axis, and the integral paths are then indented, as shown in figure 2(b).

Consider the integral

$$I = \int_{C_\pm} \frac{\mathrm{Log}\, K(\alpha)}{\alpha - y} \mathrm{d}\alpha \tag{23}$$

This integral is divided, for convenience, as

$$I = R_- + R_+ + B_- + B_+ + S_- + S_+ + Z + Y + N \tag{24}$$

R's are the contribution from the integration over larger arguments as

$$R_- = \int_{-\infty}^{-\chi_-} \frac{\mathrm{Log}\, K(\alpha)}{\alpha - y} \mathrm{d}\alpha \tag{25}$$

$$R_+ = \int_{\chi_+}^{\infty} \frac{\mathrm{Log}\, K(\alpha)}{\alpha - y} \mathrm{d}\alpha \tag{26}$$

where $\chi_\pm > \left| q_j^{\pm} \right|$.

B's are the contribution from the integration over small intervals containing the branch points:

$$B_- = \int_{b_1^-}^{b_2^-} \frac{\mathrm{Log}\, K(\alpha)}{\alpha - y} \mathrm{d}\alpha, \quad \text{with } b_1^- < q_1^- < b_2^- \tag{27}$$

$$B_+ = \int_{b_1^+}^{b_2^+} \frac{\mathrm{Log}\, K(\alpha)}{\alpha - y} \mathrm{d}\alpha, \quad \text{with } b_1^+ < q_1^+ < b_2^+ \tag{28}$$

S's are the contribution from the integration over small intervals containing the simple poles:

$$S_\pm = \sum_{n=1}^{n_c} S_n^\pm, \quad n_c \text{ being the largest propagating radial mode number} \tag{29}$$

$$S_n^- = \int_{s_{n1}^-}^{s_{n2}^-} \frac{\mathrm{Log}\, K(\alpha)}{\alpha - y} \mathrm{d}\alpha\,, \quad \text{with } s_{n1}^- < \nu_n^- < s_{n2}^- \tag{30}$$

$$S_n^+ = \int_{s_{n1}^+}^{s_{n2}^+} \frac{\mathrm{Log}\, K(\alpha)}{\alpha - y} \mathrm{d}\alpha\,, \quad \text{with } s_{n1}^+ < \nu_n^+ < s_{n2}^+ \tag{31}$$

Z's are the contribution from the integration over small intervals containing the zeroes of $K(\alpha)$:

$$Z = \sum_{n=1}^{n_o} Z_n \tag{32}$$

$$Z_n = \int_{z_{n1}}^{z_{n2}} \frac{\mathrm{Log}\, K(\alpha)}{\alpha - y} \mathrm{d}\alpha\,, \quad \text{with } z_{n1} < z_n < z_{n2} \tag{33}$$

Y is the contribution from the interval containing the pole at $\alpha = y$:

$$Y_\pm = \int_{y_1}^{y_2} \frac{\mathrm{Log}\, K(\alpha)}{\alpha - y} \mathrm{d}\alpha\,, \quad \text{with } y_1 < y < y_2 \tag{34}$$

where the plus (negative) sign indicates that the pole is above (below) the integral path. This integral needs to be evaluated only if $K(\alpha)$ is free of singularity and zeroes within the integral limit. Otherwise, it should belong to one of B, S, and Z because there are no singular points other than those involved in B, S, or Z.

Finally N is the integral over all the remaining intervals. There is no singularity at all in these intervals, and thus the integration can be carried out numerically.

$K(\alpha)$ approaches unity as $|\alpha|$ becomes large; that is, $\lim_{\alpha \to \pm\infty} K(\alpha) = 1$, and thus $K(\alpha)$ can be expanded for a large α, as

$$K(\alpha) \cong 1 + \frac{A_1}{\alpha} + \frac{A_2}{\alpha^2} \tag{35}$$

where the expansion coefficients A_1 and A_2 can be readily obtained. With this substitution to equations (25) and (26), one obtains

$$R_\pm = A_1 \left[\frac{\pm \mathrm{d}}{y \chi_\pm} \mp \frac{1}{y} \left(1 + \frac{\mathrm{d}}{y} \right) \mathrm{Log} \left(\frac{\chi_\pm - y}{\chi_\pm} \right) \right] \tag{36}$$

where

$$\mathrm{d} = \frac{A_2}{A_1} - \frac{A_1}{2} \tag{37}$$

Error limits and the expansion coefficients are used to determine the integral limits $\chi_{\pm}$.

The integral near the branch points can be replaced by

$$B_{\pm} = \int \frac{\mathrm{Log}\, Q_{\pm}(\alpha)}{\alpha - y}\mathrm{d}\alpha - \frac{1}{2}\int \frac{\mathrm{Log}(\alpha - q_1^{\pm})}{\alpha - y}\mathrm{d}\alpha \tag{38}$$

where

$$Q_{\pm}(\alpha) = K(\alpha)\cdot\sqrt{\alpha - q_1^{\pm}} \tag{39}$$

$Q_{\pm}(\alpha)$ are free of singularity and zeroes within the respective chosen integral limits.

The simple poles of $K(\alpha)$ are separated as follows:

$$S_n^{\pm} = \int \frac{\mathrm{Log}\, L_{\pm}(\alpha)}{\alpha - y}\mathrm{d}\alpha - \int \frac{\mathrm{Log}(\alpha - v_n^{\pm})}{\alpha - y}\mathrm{d}\alpha \tag{40}$$

where

$$L_{\pm}(\alpha) = K(\alpha)\cdot(\alpha - v_n^{\pm}) \tag{41}$$

$L_{\pm}(\alpha)$ are free of singularity and zeroes within the respective integral limits.

The zeroes of $K(\alpha)$ are similarly separated as

$$Z_n = \int \frac{\mathrm{Log}\, U(\alpha)}{\alpha - y}\mathrm{d}\alpha + \int \frac{\mathrm{Log}(\alpha - z_n)}{\alpha - y}\mathrm{d}\alpha \tag{42}$$

where

$$U(\alpha) = \frac{K(\alpha)}{\alpha - z_n} \tag{43}$$

$U(\alpha)$ is free of singularity and zeroes within the respective integral limit.

Now consider the integral

$$H(y)=\int_a^b \frac{\mathrm{Log}\,G(\alpha)}{\alpha-y}\,\mathrm{d}\alpha \tag{44}$$

Here $G(\alpha)$ is free of singularity and zeroes within the integral limit, and thus represents $Q_{\pm}(\alpha)$ in equation (38), $L_{\pm}(\alpha)$ in equation (40), $U(\alpha)$ in equation (42), or $K(\alpha)$ in equation (34) if $K(\alpha)$ is free of singularity in that region. This integral can be written as

$$H(y)=\int_a^b \frac{\mathrm{Log}[G(\alpha)/G(y)]}{\alpha-y}\,\mathrm{d}\alpha+\mathrm{Log}\,G(y)\int_a^b \frac{\mathrm{d}\alpha}{\alpha-y} \tag{45}$$

As α approaches y, one readily obtains

$$\frac{\mathrm{Log}[G(\alpha)/G(y)]}{\alpha-y}\cong\frac{G'(y)}{G(y)} \tag{46}$$

Thus, the first integral in equation (45) does not involve any singularity, and can be easily evaluated whether y is within the integral limit or not. The integral contained in the second term yields

$$\begin{aligned}\int_a^b \frac{\mathrm{d}\alpha}{\alpha-y_{\pm}}&=\mathrm{Log}\left(\frac{b-y_{\pm}}{a-y_{\pm}}\right),\quad \text{for}\quad y_{\pm}<a\ \text{ or }\ y_{\pm}>b\\ &=\mathrm{Log}\left(\frac{b-y_{\pm}}{y_{\pm}-a}\right)\mp i\pi,\quad \text{for}\quad a<y_{\pm}<b\end{aligned} \tag{47}$$

where $(\pm)$ signs are used to indicate that the simple pole is above (+) or below (–) the integral path, which is indented around the pole like $\cup$ for (+) and $\cap$ for (–).

Consider the integrals

$$\Omega_{-}^{-}=\int_a^b \frac{\mathrm{Log}(\alpha-\xi_{-})}{\alpha-y_{-}}\mathrm{d}\alpha \tag{48}$$

$$\Omega_{+}^{-}=\int_a^b \frac{\mathrm{Log}(\alpha-\xi_{-})}{\alpha-y_{+}}\mathrm{d}\alpha \tag{49}$$

$$\Omega_{-}^{+}=\int_a^b \frac{\mathrm{Log}(\alpha-\xi_{+})}{\alpha-y_{-}}\mathrm{d}\alpha \tag{50}$$

$$\Omega_{+}^{+}=\int_a^b \frac{\mathrm{Log}(\alpha-\xi_{+})}{\alpha-y_{+}}\mathrm{d}\alpha \tag{51}$$

Here, the singular point at $\alpha = \xi$ is within the integral limit, that is, $a < \xi_{\pm} < b$. The subscript on ξ and y is used to indicate that the pole is above (+) or below (–) the integral path. The indented integral paths are shown in figure 4. The second integral in each of equations (38), (40), and (42) is identified with one of the integrals in equations (48)–(51). These integrals are evaluated as follows:

For $y_{\pm} < a$,

$$\Omega_{\pm}^{\pm} = \mp i\pi \operatorname{Log}\left(\frac{\xi_{\pm} - y_{\pm}}{a - y_{\pm}}\right) - \frac{\pi^2}{3} + \frac{1}{2}\cdot\left[\left(\operatorname{Log}(b - y_{\pm})\right)^2 + \left(\operatorname{Log}(\xi_{\pm} - y_{\pm})\right)^2\right]$$
$$- \operatorname{Log}(\xi_{\pm} - y_{\pm})\cdot\operatorname{Log}(a - y_{\pm}) + \sum_{j=1}^{\infty}\frac{1}{j^2}\left[\left(\frac{a - y_{\pm}}{\xi_{\pm} - y_{\pm}}\right)^j + \left(\frac{\xi_{\pm} - y_{\pm}}{b - y_{\pm}}\right)^j\right] \tag{52}$$

and for $y_{\pm} > b$,

$$\Omega_{\pm}^{\pm} = \mp i\pi \operatorname{Log}\left|\frac{\xi_{\pm} - y_{\pm}}{a - y_{\pm}}\right| + \frac{\pi^2}{3} - \frac{1}{2}\cdot\left[\left(\operatorname{Log}(y_{\pm} - \xi_{\pm})\right)^2 + \left(\operatorname{Log}(y_{\pm} - a)\right)^2\right]$$
$$+ \operatorname{Log}(y_{\pm} - \xi_{\pm})\cdot\operatorname{Log}(y_{\pm} - b) - \sum_{j=1}^{\infty}\frac{1}{j^2}\left[\left(\frac{y_{\pm} - b}{y_{\pm} - \xi_{\pm}}\right)^j + \left(\frac{y_{\pm} - \xi_{\pm}}{y_{\pm} - a}\right)^j\right] \tag{53}$$

where the upper (lower) sign of $i\pi$ corresponds to ξ_+ (ξ_-).

For $a < y_{\pm} < b$,

$$\Omega_{-}^{\pm} = \pm i\pi \operatorname{Log}(y_- - a) + i\pi\left[-\operatorname{Log}(y_- - \xi_{\pm}) \mp \operatorname{Log}(y_- - \xi_{\pm})\right]$$
$$-\frac{1}{2}\left[\left(\operatorname{Log}(b - \xi_{\pm})\right)^2 + \left(\operatorname{Log}(y_- - a)\right)^2\right] + \operatorname{Log}(b - \xi_{\pm})\cdot\operatorname{Log}(b - y_-) \tag{54}$$
$$+\frac{\pi^2}{2} - \sum_{j=1}^{\infty}\frac{1}{j^2}\left[\left(\frac{y_- - \xi_{\pm}}{b - \xi_{\pm}}\right)^j + \left(\frac{y_- - \xi_{\pm}}{y_- - a}\right)^j\right]$$

$$\Omega_{+}^{\pm} = \pm i\pi \operatorname{Log}(y_+ - a) + i\pi\left[\operatorname{Log}(y_+ - \xi_{\pm}) \mp \operatorname{Log}(y_+ - \xi_{\pm})\right]$$
$$-\frac{1}{2}\left[\left(\operatorname{Log}(b - \xi_{\pm})\right)^2 + \left(\operatorname{Log}(y_+ - a)\right)^2\right] + \operatorname{Log}(b - \xi_{\pm})\cdot\operatorname{Log}(b - y_+) \tag{55}$$
$$+\frac{\pi^2}{2} - \sum_{j=1}^{\infty}\frac{1}{j^2}\left[\left(\frac{y_+ - \xi_{\pm}}{b - \xi_{\pm}}\right)^j + \left(\frac{y_+ - \xi_{\pm}}{y_+ - a}\right)^j\right]$$

All the integrals involving singular points are analytically evaluated according to equations (47) and (52)–(55). For large arguments extending to the infinite, the integral is evaluated according to equation (36). The rest involves finite integrals with well-behaved integrands, and thus can be numerically evaluated without any difficulty.

A remark will be made on the results in equations (54) and (55), particularly on the second term on the right. This term vanishes if y and ξ are on the same side (above or below) with respect to the integral path. However, if y and ξ are separated by the integral path, the second term equals $\pm 2\pi i \,\mathrm{Log}(y_{\pm} - \xi_{\mp})$ and diverges as y approaches ξ. Of the K-factors contained in the results in equations (17) and (19), only $K_+(-\eta(\theta))$ can have y and ξ separated by the integral path. Its argument is above the integral path according to equation (15). As θ varies, the argument can approach a singular point located below the integral path. For this case, the second term above is given by $2\pi i \,\mathrm{Log}(-\eta(\theta) - \xi_-)$, where ξ_- is ν_n^- or q_1^-. Inspecting equations (15), (23), (24), (38), and (55), one obtains, for $-\eta(\theta)$ close to q_1^-,

$$K_+(-\eta(\theta)) \propto \frac{1}{\sqrt{-\eta(\theta) - q_1^-}} \tag{56}$$

Similarly, from equations (15), (23), (24), (40), and (55), one obtains, for $-\eta(\theta)$ close to ν_n^-,

$$K_+(-\eta(\theta)) \propto \left(-\eta(\theta) - \nu_n^-\right)^{-1} \tag{57}$$

It follows that, as $\eta(\theta)$ approaches k_{mn}^+, then $f_{m\ell}(\theta)$ given in equation (19) tends to be zero for $n \neq \ell$ and will reach the maximum for $n = \ell$. Also, one can see that $f_{m\ell}(\theta)$ will remain finite as $\eta(\theta)$ approaches $k_1/(1 + M_1)$, as discussed earlier.

CONCLUDING REMARKS

An analysis for evaluation of the Wiener-Hopf solution was presented for sound radiation from an unflanged circular duct with mean flows. This analysis was initially developed for radiation of spinning modes in conjunction with aircraft inlet noise control studies. We have a well-working computer code available for such radiation. However, while generating numerical results for the benchmark problems, we learned that the code needed to be refined for radiation of the axisymmetric modes.

REFERENCES

1. Levine, H.; and Schwinger, J.: On the Radiation of Sound from an Unflanged Circular Duct. Phys. Rev., vol. 73, 1948, pp. 383–406.

2. Weinstein, L. A.: The Theory of Diffraction and the Factorization Method. Golem Press, 1969.

3. Savakar, S. D.: Radiation of Cylindrical Duct Acoustic Modes with Flow Mismatch. J. Sound and Vibration, vol. 42, 1975, pp. 363–386.

4. Cho, Y. C.: Rigorous Solutions for Sound Radiation from Circular Ducts with Hyperbolic Horns or Infinite Plane Baffle. J. Sound and Vibration, vol. 69, 1980, pp. 405–425.

5. Noble, B.: Methods based on the Wiener-Hopf Techniques. Pergamon Press, 1958.

6. Cho, Y. C.: Reciprocity Principle in Duct Acoustics. J. Acoustical Soc. Am., vol. 67, 1980, pp. 1421–1426.

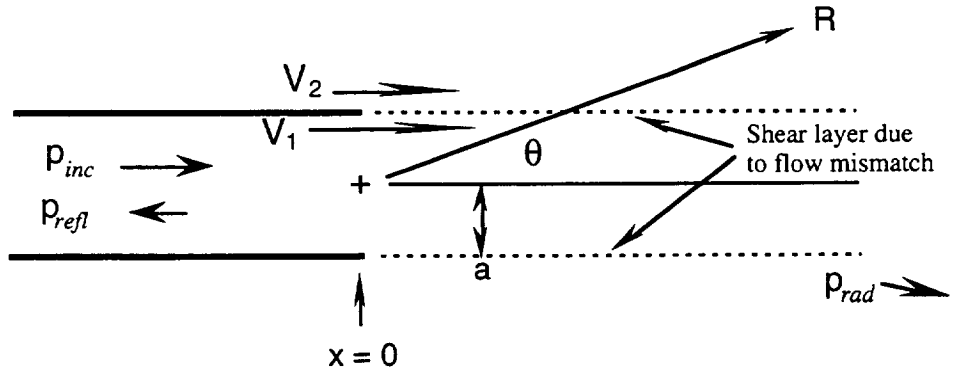

Figure 1. Sound radiation from unflanged circular duct with flow.

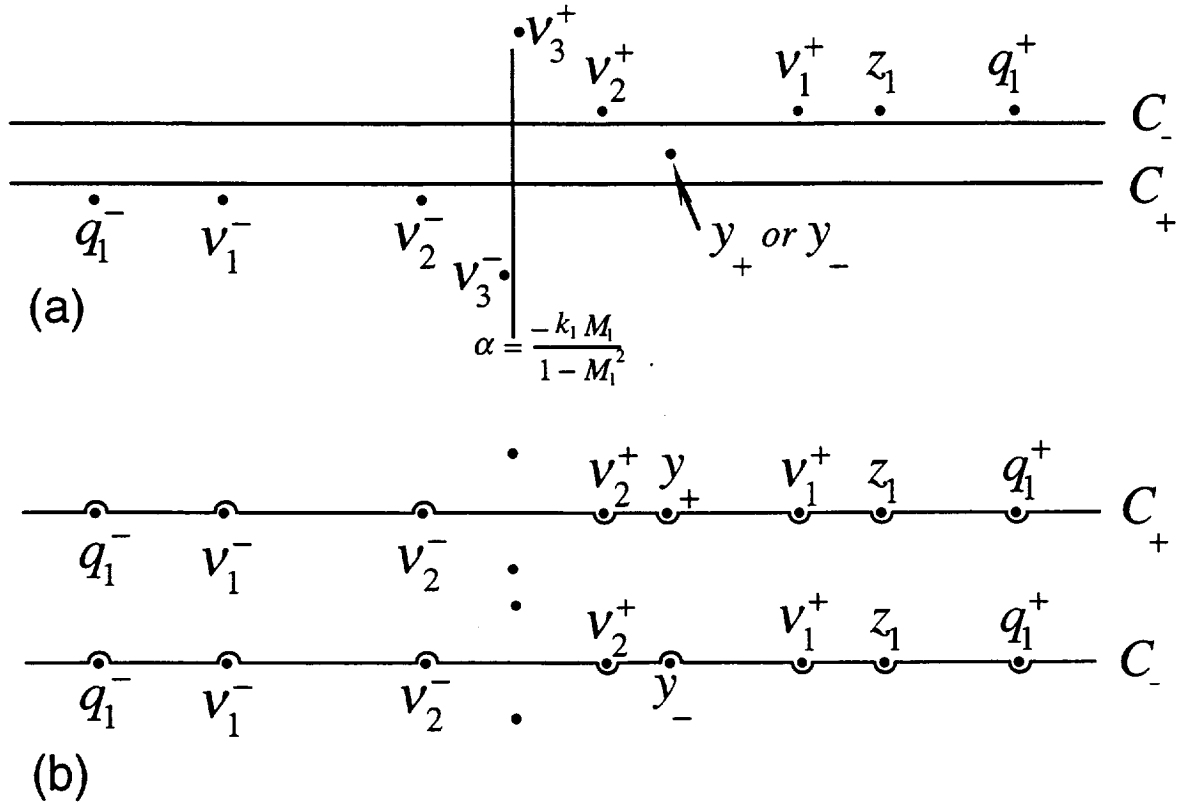

Figure 2. (a) Integral paths C_+ and C_- and singular points ($\nu_3^{\pm}$ corresponds to an attenuating mode); (b) indentation of the integral paths as $\mathcal{Im}(k) \rightarrow$ approaches 0.

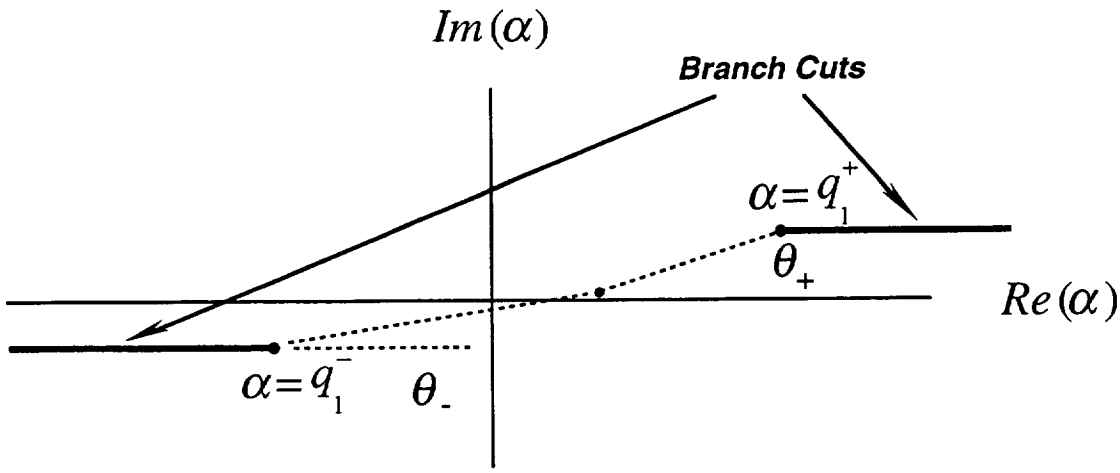

Figure 3. Branch points, branch cuts, and phase convention: $0° < \theta_- < 180°$ and $-180° < \theta_+ < 0°$.

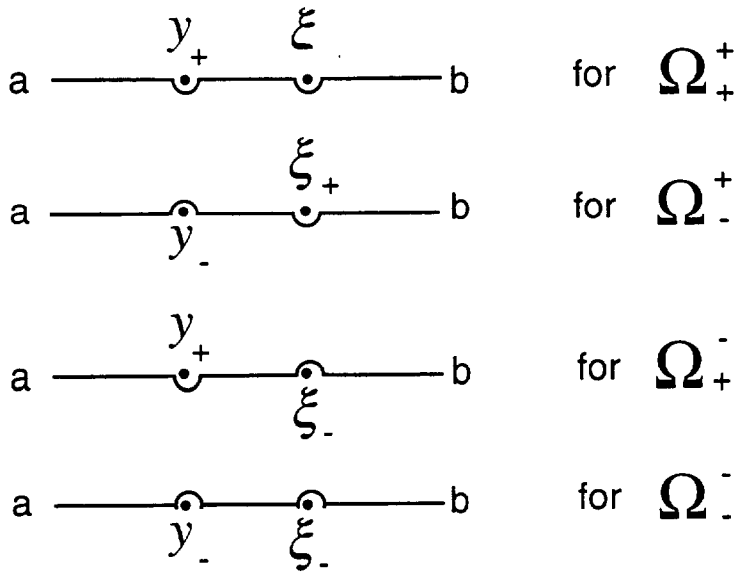

Figure 4. Integral path indentation for integrations involving two singular points at $\alpha = y$ and ξ.

REPORT DOCUMENTATION PAGE

Form Approved
OMB No. 0704-0188

1. AGENCY USE ONLY *(Leave blank)*	2. REPORT DATE	3. REPORT TYPE AND DATES COVERED
	June 1997	Technical Memorandum

4. TITLE AND SUBTITLE

Exact Solutions for Sound Radiation from a Circular Duct

5. FUNDING NUMBERS

632-30-34

6. AUTHOR(S)

Y. C. Cho and K. Uno Ingard[†]

7. PERFORMING ORGANIZATION NAME(S) AND ADDRESS(ES)

Ames Research Center
Moffett Field, CA 94035-1000

8. PERFORMING ORGANIZATION REPORT NUMBER

A-976769

9. SPONSORING/MONITORING AGENCY NAME(S) AND ADDRESS(ES)

National Aeronautics and Space Administration
Washington, DC 20546-0001

10. SPONSORING/MONITORING AGENCY REPORT NUMBER

NASA TM-112200

11. SUPPLEMENTARY NOTES

Point of Contact: Y. C. Cho, Ames Research Center, MS 269-3, Moffett Field, CA 94035-1000
(415) 604-4139
[†]Massachusetts Institute of Technology, Cambridge, MA 02139

12a. DISTRIBUTION/AVAILABILITY STATEMENT

Unclassified — Unlimited
Subject Category 01

12b. DISTRIBUTION CODE

13. ABSTRACT ***(Maximum 200 words)***

This paper presents a method of evaluation of Wiener-Hopf technique solutions for sound radiation from an unflanged circular duct with infinitely thin duct wall, including mean flows.

14. SUBJECT TERMS

Sound radiation, Wiener-Hopf technique, Circular ducts

15. NUMBER OF PAGES

18

16. PRICE CODE

A03

17. SECURITY CLASSIFICATION OF REPORT	18. SECURITY CLASSIFICATION OF THIS PAGE	19. SECURITY CLASSIFICATION OF ABSTRACT	20. LIMITATION OF ABSTRACT
Unclassified	Unclassified		